Globally optimal tool paths for sculptured surfaces with emphasis to machining error and cutting posture smoothness

Nikolaos A. Fountas[1-3], Nikolaos M. Vaxevanidis[1]*, Constantinos I. Stergiou[2,3], Redha Benhadj-Djilali[3]

[1]*Laboratory of Manufacturing Processes and Machine Tools (LMProMaT), Department of Mechanical Engineering Educators, School of Pedagogical and Technological Education (ASPETE), ASPETE Campus, N. Heraklion, GR 141 21 Athens, Greece*

[2] *Department of Engineering, University of West Attica (UNIWA), Egaleo Campus, GR 122 44, Athens, Greece*

[3]*Faculty of Science, Engineering and Computing (SEC), Kingston University, Roehampton Vale Campus, Friars Avenue, Kingston upon Thames, London SW15 3DW, UK*

Global optimization for manufacturing problems is mandatory for obtaining versatile benefits to facilitate modern industry. This paper deals with an original approach of globally optimizing tool paths to CNC-machine sculptured surfaces. The approach entails the development of a fully automated manufacturing software interface integrated by a non-conventional genetic/evolutionary algorithm to enable intelligent machining. These attributes have been built using already existing practical machining modelling tools such as CAM systems so as to deliver a truly viable computer-aided manufacturing solution. Since global optimization is heavily based in the formulation of the problem, emphasis has been given to the definition of optimization criteria as crucial elements for representing performance. The criteria involve the machining error as a combined effect of chord error and scallop height, the tool path smoothness and productivity. Experiments have been designed considering several benchmark sculptured surfaces as well as tool path parameters to validate the aforementioned criteria. The new approach was implemented to another sculptured surface which has been extensively tested by previous research works. Results were compared to those available in the literature and it was found that the proposed approach can indeed constitute a promising and trustworthy technique for the global optimization of sculptured surface CNC tool paths.

Keywords: sculptured surfaces; cnc machining; tool path optimization; genetic algorithms; manufacturing software; metaheuristics

1.Introduction

Sculptured surface machining constitutes a material removal process capable of achieving significant improvements concerning manufacturing efficiency and surface finish. The application of several configurations of 5-axis CNC machine tools has helped reducing machining time of sculptured surfaces, attaining larger material removal rates and allowing larger tool accessibility range. Many advantages of employing proper cutting tool geometries combined to the 5-axis machining technology have also been reported with emphasis to toroidal end-mills due to their efficiency (Redonnet et al 2016; Redonnet et al. 2013). Unlike 3-axis surface machining where the process of generating cutting tool paths is quite straightforward owing to vertical Z-axis orientation, 5-axis tool paths introduce great challenge to practical machinists for determining proper values for tool path parameters.

A noticeable number of sculptured surface tool path optimization approaches have optimal tool positioning as their primary objective. Their philosophy is based on the sequential configuration of cutter location (CL) points to be met by cutting tools as they interpolate the designed surface under a preset cut tolerance. In addition the possibility of producing larger machining strips by simultaneously maintaining scallop height al low levels is also an essential objective for tool positioning strategies. Early research works include the proposals of Vickers and Quan (1989); Jensen and Anderson (1993) as well as Rao, Ismail and Bedi (1997) concerning the "Principal Axis Method (PAM). Warkentin, Ismail and Bedi (2000a and 2000b) proposed the "Multi-point machining (MPM) method; whilst Gray, Bedi and Ismail (2003) and Gray, Bedi and Ismail (2005) proposed "Rolling ball" and "Arc-Intersect" tool positioning methods respectively. Recent contributions for tool positioning are found in the work of Fan et al. (2013) who implemented their "rotary contact" approach for the 5-axis machining of sculptured surfaces. Their method rotates the tool backward according to an offset surface instead of the true one resulting thus to larger machining strips. However their approach has been fully exploited for the case of convex surfaces only. Gan et al. (2016) studied the optimal direction that a cutting tool should rotate around so as to produce wider machining strips by implementing the "mechanical equilibrium" for the

creation of iso-parametric tool paths. Redonnet et al. (2016) presented a tool positioning strategy for 3-axis sculptured surface CNC machining using a toroidal cutting tool. Their work benefits from the milling of "parallel-planes" and the effective cutting shape of filleted end-mills to achieve larger machining strips whilst simultaneously maintaining low scallop height.

New generation computer-aided manufacturing (CAM) systems play an important role in formulating reliable tool paths for 5-axis sculptured surface machining and are in fact the only practical tool where several scenarios may be tested to judge tool path efficiency. By taking into account the properties of modern CAM systems as well as their open architectures (APIs) allowing for further customization via programming, several researchers have developed new methodologies for accurate tool path generation based on performance metrics being directly evaluated using CAM software. Two representative process-related criteria investigated are cutting forces (Lamikiz et al. 2005; Lopez de Lacalle et al. 2005; Zeroudi, Fontaine and Necib, 2012) and material removal rate (Moodleah and Makhanov 2015). Xu et al. (2010) proposed an approach integrating a commercially available CAM system to create successive cutter contact points for sculptured surface tool paths as the tool is controlled by two drive-curves. First their approach generates tool points for the major curve and according to the cut tolerance another set of points is obtained for the second curve maximizing thus the machining strip.

The goal of suggesting intelligent tool path generation is to facilitate the engineers' tedious decision making tasks in terms of providing values for tool path parameters, whilst; an important reason for suggesting optimality in tool path generation is the reduction of time-consuming processes that follow finish-machining such as polishing. Agrawal, Pratihar and Choudhury (2006) applied a genetic algorithm to generate tool paths for sculptured surfaces such that equal scallops would be produced. Ulker, Turanalp and Halkaci (2009) implemented an artificial immune algorithm to generate CC points comprising the tool path according the preset error in the case of 3-axis surface machining. Manav, Bank and Lazoglu (2013) established a triple-bounded problem for the sculptured surface machining problem involving mean scallop height, machining time and mean cutting force. Instead of sequentially creating locally optimal CC points and adjacent tool passes Djebali et al. (2015) captured the need for global optimization and they presented a multi-objective optimization approach involving scallop height and minimum path length for 3-axis milling. Lu, Ding and Zhu (2017) presented an intelligent methodology for optimizing the whole tool path in the case of 5-axis surface machining. A differential evolution (DE) algorithm handled maximal curvature of tool path curve; feed direction change; tool path curve smoothness and tool orientation angles as optimization criteria. Their methodology was tested on a widely-examined benchmark sculptured part. To deal with the generalized part quality inspection problem, Mohammad et al., (2018) reviewed optimization approaches in a multi-stage manufacturing system. Amaral (2018), targeted on implementing a mixed-integer programming module so as to deal with manufacturing problems such as the sculptured surface machining problem investigated in this paper. An ongoing research is also observed in the development of modern meta-heuristics for optimization like the hybrid discrete bat algorithm of Chansombat et al., (2018).

2. Research problems, contribution and original aspects

Sculptured surface machining is a well-established research area for which many different strategies are available for implementation. Referring to tool path optimization methodologies based on tool positioning noticeable limitations exist in terms of their computational algorithms and their finite mathematical restrictions. Despite the fact that selection of roughing and 3-axis finishing tool paths is more obvious, a question rises concerning the proper choice of a tool positioning strategy since multiple selections can be applied for the same task. Assuming that assistance is provided in terms of a specific tool positioning strategy selection, related parameters would yet to be determined by machinists either by consulting special manuscripts or by trial-and-error experiments. Another limitation characterizing such approaches is their lack of global optimization capabilities owing to the sequential creation of crucial tool path instances (i.e. CL points or adjacent tool passes) by considering tool inclination, forward step and cutting tolerance. Beyond the widely accepted fact that multiple local optimum results do not necessarily deliver a globally optimal solution, inaccuracies among neighboring tool path instances might violate constraints owing to the 'one-at-a-time' computations without taking into account previous locally optimal instances.

A significant flaw concerning optimal tool path creation is also observed to the establishment of optimization criteria as crucial quality objectives for optimization given in the form of objective functions for intelligent algorithms. Most of these objective functions are developed under the scope of providing a physical relationship between independent variables (tool path parameters) and dependent responses (optimization criteria). Such attempts would inevitably lack of generalization since empirical models are often valid only to sculptured parts been previously used for designing experiments from which such models are finally obtained. Another important research question concerning optimization criteria employed for optimizing a process is to what extend the criteria reflect the overall problem thus constituting trustworthy attributes to warrant evaluation for global optimization. Since the quality of a solution is not only depended from the robustness of an intelligent algorithm or an expert system but also to the problem formulation, optimization criteria ought to include local information, yet; their expression should lead to a globally optimal outcome. The gaps of the existing research are summarized as follows:

- Several tool positioning strategies are available for the same task; however their selection criteria are ambiguous.
- Paths created by tool positioning strategies depend on the restrictions and properties of their corresponding computation approaches. Therefore resulting tool paths cannot ensure global optimality requirements.
- Despite the sophisticated notion of most modern tool path generation strategies in terms of optimization, still end-users have to traditionally determine values for their process parameters and perform trial-and-error scenarios.
- Optimization criteria should support the problem's global assessment whilst simultaneously considering local variations.

Major themes of intelligent machining are automation, simulation and optimization (Li, Lee and Gao 2015). In order to contribute to the ongoing research for achieving intelligent sculptured surface tool path optimization this work aims at presenting a fully automated; generic methodology integrated by an intelligent algorithm for the optimization of sculptured surfaces. In the proposed methodology, tool path preparation is conducted using CAM software. Instead of precisely specifying parameter values for sculptured surface tool paths, machinists are to determine only their lower and upper bounds. The parameters involved are valid to any type of tool path and are the type of cutting tool, the step over, lead and tilt angles and maximum discretization step. New criteria representing superficial quality and productivity are employed to globally reflect the resulting outputs for the optimization process whilst they formulate a triple-bounded objective according to "Pareto" approach. The methodology proposed addresses the aforementioned research limitations through its original perspectives summarized below:

- The methodology optimizes tool paths after their generation in CAM and not by sequentially formulating them by one CL point at a time or by one path at a time (local optimality);
- The methodology comprises global optimization criteria, yet; including significant local information dynamically retrieved by a CAM system;
- No user interaction is needed for determining tool path parameters during the optimization process owing to the existence of an intelligent algorithm.

3. Quality objectives identification

In sculptured surface CNC machining, cutter location as well as orientation vary along the multi-axis tool path with respect to the part surface. Consecutively the values of tool path parameters; stepover, lead and tilt angles and maximum discretization step, alter the resulting work piece-engagement boundaries at each of cutter contact points; suggesting different tool path postures. Cutter location data formulate a *mxn* pattern of points covering the entire sculptured surface represented in the *u, v* parametric space. A unique cutter location (CL) point is determined as CLP(*x, y, z, i, j, k, c1, c2*), where (*x, y, z*) are the coordinates of the machining axis system (G54) whilst (i, j, k) is the unit normal vector representing the tool's position for that CLP. Finally, c1 and c2 are the two principal curvatures of the surface for u and v respectively, responsible for the tool's inclined position to the CLP.

The aforementioned instances play crucial role to a multi-axis tool path definition since they affect the entire machining operation in terms of quality and productivity. In this paper the average values of machining error (as a combined effect of chord error and scallop height); tool path smoothness (in terms of the machining error uniformity) and the total number of cutter location data have been defined as the objectives to present a generic optimization methodology for the sculptured surface machining problem.

3.1 Chord error and scallop height estimation

Tool positioning is greatly affected by the values given for the tool path planning parameters as well as the type of cutting tool geometry with reference to the surface's geometrical properties in the case of sculptured surface machining. When it comes to cutting tool selection, one may distinguish among ball end; flat end and filleted end-mills, whilst an important geometrical property of a surface is the local curvature varying depending on the CL point to which the tool is positioned. As the tool follows the tool path towards feed direction, it subsequently meets cutter location points with the consequence of producing sequential chord errors whose magnitude depends on the distance L_i between two cutter location points and the local curvature ρ_i existing in between the two unit normals $\overrightarrow{n_1}$ and $\overrightarrow{n_2}$ determined with respect to the first CLP and the second CLP respectively. 3D distances L_i corresponding to the lengths of chords connecting the pairs of consecutive CLPs by considering the machining axis system in Cartesian space, are computed using Equation 1 (Fisher 1989).

$$L_i = \sqrt{\left(x_{i+1} - x_i\right)^2 + \left(y_{i+1} - y_i\right)^2 + \left(z_{i+1} - z_i\right)^2} \quad (1)$$

Subsequent local curvatures may be computed by employing vector algebra and retrieving dot products of normal vectors utilizing the angle between them. Thereby, with reference to the two unit normals $\vec{n_1}$ and $\vec{n_2}$, the angle θ is determined as, $\theta = \arccos(\vec{n_1} \circ \vec{n_2})$, whereas local curvatures ρ_i (mm^{-1}) are finally computed by using Equation 2.

$$\rho_i = 2 \times \sin(\theta / 2) / L_i \quad (2)$$

With the help of the aforementioned computations, consecutive chord errors C_e (mm) are calculated by employing Equation 3.

$$C_e = \rho_i - \sqrt{\rho_i^{\,2} - \left(\frac{L_i}{2}\right)^2} \quad (3)$$

At each CLP the tool's positioning yields variable effective cutting postures which in turn result to significant fluctuations of scallop height. Equation 4 (Redonnet et al. 2013; Segonds et al. 2017), was applied to compute R_{Eff} for flat-end; fillet-end and ball-end mills. Note that for ball end-mills, R_{Eff} is not affected by tool inclination angles in 5-axis machining.

$$R_{eff}\begin{bmatrix} Flat-end \\ Toroidal \\ Ball-end \end{bmatrix} = \begin{Bmatrix} \dfrac{R \times \cos^2 a_T}{\sin a_L \times \left(1 - \sin^2 a_T \times \sin^2 a_L\right)} \\ \dfrac{(R-r) \times \cos^2 a_T}{\sin a_L \times \left(1 - \sin^2 a_T \times \sin^2 a_L\right)} + r \\ R \end{Bmatrix} \quad (4)$$

where:

R_{eff} : the effective cutting radius given the tool inclination;

R : the cutter's radius;

r : the cutter's corner radius for toroidal end-mills;

a_L : lead angle in degrees;

a_T : tilt angle in degrees.

By considering the latest research for scallop height estimation (Segonds et al. 2017) owing to step over parameter, the magnitude of scallop height sh_{a_e}, was computed using Equation 5.

$$sh_{a_e} = R_{eff} - \sqrt{R^2_{\,eff} - \frac{a_e^{\,2}}{4}} \quad (5)$$

In Equation 5, R_{eff} is the effective cutting radius computed according to a given cutting tool's geometrical configuration and a_e is the stepover distance between passes, in mm. Although the relation among effective radii and scallop heights has been successfully realized (Redonnet et al. 2013; Segonds et al. 2017) no research has been conducted to experimentally verify it and finally deploy it as an essential attribute in taking part to the formulation of crucial objectives for testing optimization potentials in sculptured surface machining.

3.2 Uniform tool orientation for tool path smoothness

Tool path smoothness in sculptured surface machining is an important criterion for which few research efforts are found in literature. For a multi-axis tool path to maintain smooth cutting, tool positioning variation throughout the entire sculptured surface should be minimized, yet; not at the expense of part quality in terms of gouging. Indeed, tool

axis variation is necessary to avoid undercuts when the surface fluctuates strongly towards feed direction. However it is impossible for the engineer to capture the exact values for the inclination angles so that tool path smoothness and gouge avoidance will be simultaneously achieved.

To judge tool path smoothness, machining error distribution has been examined for each CLP after the tool path computation with reference to the tool orientation and the rest of tool path parameters mentioned above. Standard deviation of local machining error distributions can reflect a way in which the excess material is distributed on the ideally designed surface and for this reason it has been selected in this study as the performance metric representing tool path smoothness. An important prerequisite for enabling this computation is to compute the machining error as the sum of the average value of all local errors corresponding to subsequent CLPs and the average value of all scallop heights. Note that the averages of chord error and scallop height are the true means since all CLPs are considered rather than a sample of them (Fard and Feng 2011; Mordkoff, 2015).

Let C_{e_i} be the chord error between two consecutive CLPs and h_i to be the scallop height at *i*th CLP. Obviously the total number of chord errors will be equal to the number of CLPs minus one (since a pair of two CLPs yields one chord error); whilst the total number of scallops will be equal to the number of successfully generated CLPs constituting the tool path. In either case the mean, the mean differences, the variance and the standard deviation will be given by the known statistical formulas given in Equations 6; 7, 8 and 9 respectively.

$$\overline{x} = \frac{1}{\nu} \cdot \sum_{i=1}^{\nu} x_i \tag{6}$$

$$\overline{x}\_diff = \frac{1}{\nu} \sum_{i=1}^{\nu} \left| x_i - \overline{x} \right| \tag{7}$$

$$s^2 = \frac{1}{\nu - 1} \cdot \sum_{i=1}^{\nu} (x_i - \overline{x})^2 = \frac{1}{\nu(\nu - 1)} \left(\nu \cdot \sum_{i=1}^{\nu} x_i^2 - \left(\sum_{i=1}^{\nu} x_i \right)^2 \right) \tag{8}$$

$$s = \sqrt{\frac{1}{\nu - 1} \cdot \sum_{i=1}^{\nu} (x_i - \overline{x})^2} = \sqrt{\frac{1}{\nu(\nu - 1)} \left(\nu \cdot \sum_{i=1}^{\nu} x_i^2 - \left(\sum_{i=1}^{\nu} x_i \right)^2 \right)} \tag{9}$$

By deploying the property of machining error distribution as a quality objective via the standard deviation to assess tool path smoothness, the error's variability and local fluctuations are quantified for the entire tool path with reference to resulting tool orientations at all CLPs comprising it.

3.3 Objectives validation

To examine the applicability of relations presented in Equations 3 and 5 (chord error and scallop height estimation), a series of full factorial experimental designs were established and conducted by adopting four benchmark sculptured surfaces imposing different challenges when it comes to tool path planning. Figure 1a shows an open type bi-cubic Bezier surface (Gray, Bedi and Ismail 2003); Figure 1b shows a multivariable test surface (Manav, Bank and Lazoglu 2013); Figure 1c shows a complex-curvature surface (Roman et al. 2015) and Figure 1d shows a challenging sculptured surface with two Bezier patches mirrored using a C0 continuous curve (Gray, Ismail and Bedi 2004). The surfaces depicted in Figure 1 are designated as SS-1; SS-2; SS-3 and SS-4 for easy reference in the paper. To virtually machine these surfaces, flat end and filleted end-mills were considered, employing a multi-axis sweeping tool path. Prior investigation was conducted to determine the applicable ranges for the tool path planning parameters with regard to the properties of the selected benchmark surfaces.

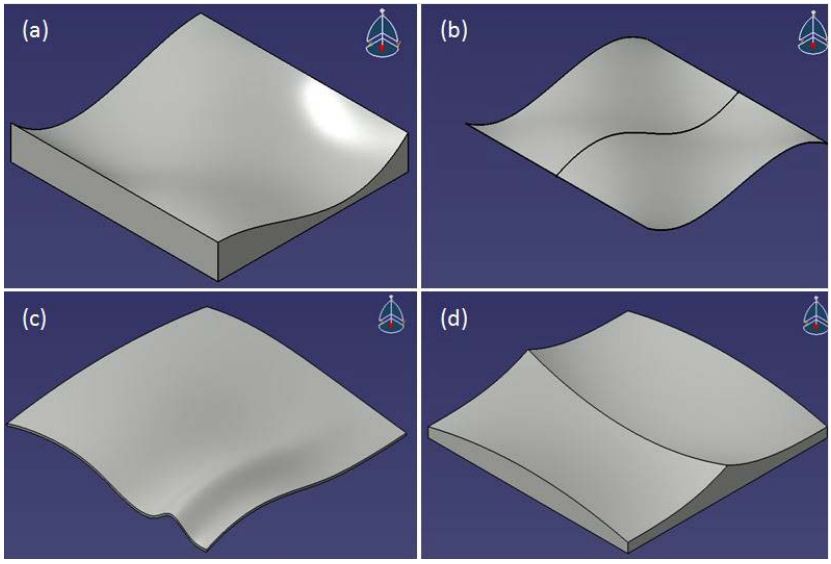

Figure 1. Benchmark sculptured surfaces to examine the validity of quality objectives selected: (a) SS-1; (b) SS-2; (c) SS-3; (d) SS-4.

Apart from the examination of the relations presented to formulate the quality objectives for the sculptured surface machining problem, the experimental results were studied to capture the trend of main effects and interactions among tool path parameters for surfaces with different geometrical properties. This contributes to the construction of tool path chromosomes to be later evaluated by an artificial intelligent system, i.e.; a genetic algorithm, in their binary representation form.

The machining experiments per sculptured surface were conducted in *Dassault Systemes CATIA® V5 R18* advanced machining workbench. A programming function (CAD-CAM interaction routine) was developed in Visual Basic® 6 that undertakes the automatic tool path planning with different parameter values and all computations necessary to obtain the results for the performance objectives. Table 1 shows the tool path parameters as well as their corresponding levels for all individual full factorial (2^5-L_{32}) experimental designs.

Table 1. Experimental designs with tool path parameters and corresponding levels according the benchmark surface tested.

Benchmark surface	Levels	Tool	Step over (%D)	Lead angle (deg)	Tilt angle (deg)	MaxDstep (mm)
SS-1	Low	D37.4-Rc0	10	20	0	0.007
	High	D37.4-Rc6	45	35	7	1.397
SS-2	Low	D12-Rc0	17	15	0	1
	High	D12-Rc3	45	20	15	5
SS-3	Low	D20-Rc0	10	30	0	0.5
	High	D20-Rc4	45	40	5	2.5
SS-4	Low	D50.8-Rc6.35	10	15	0	0.762
	High	D50.8-Rc0	45	20	15	2

Machining simulation experiments for all surfaces, involved the following steps.

- Automatic tool path computation according to the inputs for the parameters corresponding to the “multi-axis sweeping” tool path style;
- CAD-intersection routine execution to automatically compute the average values of mean chord error and mean scallop height;
- Machining simulation and storage of 3D CAM outputs in *.stl file format;
- Real-time deviation measurements (with respect to ideal surfaces), performed on scallop volumes of 3D CAM outputs in their *.stl version using 3D metrology utilities of *Geomagic® Qualify Probe® 2013*;
- Export of real-time deviation measurements for scallop height in *.txt format;
- Correlation examination among analytical and real-time scallop height measurements.

A very good correlation has been observed among the analytically computed means of scallop height values and those experimentally measured using real-time 3D surface deviation tools of *Geomagic® Qualify Probe® 2013*. A two-sample t-test was also conducted to examine the statistical significance among differences of experimental and

analytical results. The results ensure that the analytical expression employed to compute the objective of scallop height can be involved to the final fitness function formulation for optimizing the sculptured surface machining problem with the use of an intelligent algorithm. Figure 2 illustrates the comparative diagrams obtained by correlating the analytical mean scallop height results and those experimentally measured using real-time 3D surface deviation for SS-1; SS-2; SS-3 and SS-4 respectively (Figure 2a to 2d) along with p-values from the two-sample t-test conducted. Results of mean chord errors have been verified by implementing the routine developed for finding local curvatures (and consecutively chord errors) was verified by comparing analytical outputs to those obtained by manually measuring several experimental free-form models via the "*Surfacic curvature analysis*" tool of *Dassault Systemes CATIA® V5 R18*.

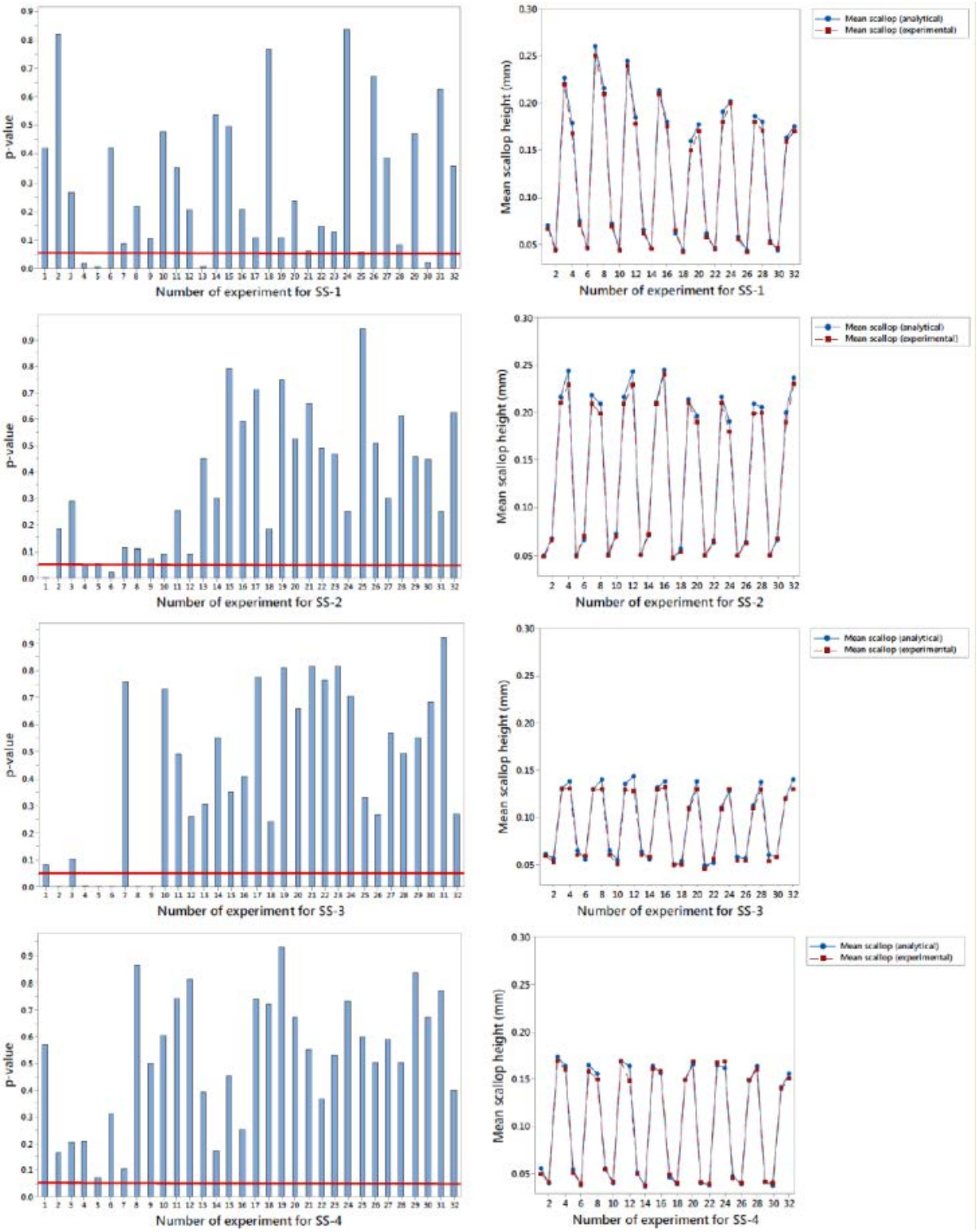

Figure 2. Comparative diagrams and statistical significance between analytical and real-time measured mean scallop heights using 3D CAM outputs from machining simulations: (a) SS-1; (b) SS-2; (c) SS-3; (d) SS-4.

The experiments conducted, followed by a statistical analysis to examine the effects of tool path parameters on the objectives of mean scallop height; mean chord error, standard deviation of scallop; standard deviation of chord error and finally the number of CLPs for tool paths. This analysis has been conducted to all four benchmark sculptured surfaces and it was shown that no standard trend of influence can be considered when it comes to tool path planning for sculptured surfaces. Tool path parameters differently affect the aforementioned performance metrics with respect to different geometrical properties of sculptured surfaces. This leads to the conclusion than the optimization problem corresponding to sculptured surface machining ought to be dynamically solved by directly considering the automation capabilities of new generation's CAD-CAM systems via their application programming interface (API) whilst regression modelling might jeopardize the optimization process when mathematical expressions are used as fitness functions. Another important observation from the experimental procedure described above is that the binary structure of candidate solutions should be properly formulated by taking into account the variability in terms of the effects of tool path parameters on the objectives and the formulation of the objective function itself.

3.5 Objective function formulation

Apart from presenting non-dominated solutions appeared to a Pareto-front for two or three optimization objectives, a tendency to present a single multi-objective result is noticed (Manav et al. 2013) because practitioners may prefer one Pareto optimal output from many; depending the preferences and the problem's properties. The weighted sum method (Fountas et al. 2017; Lu, Ding and Zhu 2017; Manav, Bank and Lazoglu 2013) has been employed to couple the criteria of mean machining error (chord error and scallop height) mean standard deviation of the error and number of CLPs and make them comparable at the same level by properly articulating their common impact via normalization. The computation formula giving the weighted sum among the three criteria is shown in Equation 10 where ff_S refers to the single objective (fitness function); $norm\_\overline{h}$ expresses the normalized mean scallop height; $norm\_\overline{C_e}$ expresses the normalized mean chord error; $norm\_\overline{stdevh}$ expresses the normalized mean standard deviation of scallop; $norm\_\overline{stdevC_e}$ represents the normalized mean standard deviation of chord error and $NoCLs$ expresses the total number of CLPs comprising a tool path.

$$ff_S = \left[(norm\_\overline{h} + norm\_\overline{C_e}) + (norm\_\overline{stdevh} + norm\_\overline{stdevC_e}) + norm\_NoCLs \right] \quad (10)$$

The proposed methodology supports also the non-dominated solutions concept represented through the application of a 3D Pareto front where each axis suggests an optimization criterion. As such, the triple-bounded problem is also evaluated by adopting the objective function represented in Equation 11. In Equation 11, ff_P represents the "Pareto" objective function.

$$ff_P = \sqrt{(norm\_\overline{h} + norm\_\overline{C_e})^2 + (norm\_\overline{stdevh} + norm\_\overline{stdevC_e})^2 + norm\_NoCLs^2} \quad (11)$$

4. Intelligent methodology for optimal tool path generation

By considering the impact of tool path parameters (cutting tool; step over; lead angle; tilt angle and maximum discretization step), combinations with regard to parameters' values are treated as candidate solutions (tool path "chromosomes") which are presented as binary-encoded numerical sequences. Thereby, binary-encoded candidate solutions are mapped to their corresponding phenotypes to enable their evaluation by the intelligent algorithm that integrates the methodology proposed. The entire process for optimizing tool paths for sculptured surface machining is facilitated by implementing an automation function responsible for interacting with the intelligent algorithm and automating the CAD-CAM environment's utilities. Multi-objective optimization is achieved using a virus-evolutionary genetic algorithm (MOVEGA) that adheres to the natural procedure of viruses to copy and/or transmit their genome from generation to generation of individuals through viral infection. Such a sophisticated approach is yet to be fully realized and applied to solve multi-objective optimization problems related to manufacturing and production. Nevertheless some noticeable contributions related to the philosophy of this different algorithm as well as its successful engineering applications have already presented interesting results (Fountas et al. 2017; Lu et al. 2017; Liang and Juarez 2016; Kubota, Fukuda and Shimojima, 1996).

4.1 Tool path chromosome structure and intelligent operators

Candidate solutions (tool path chromosomes) are appeared as binary-encoded sequences with regard to the selected values of tool path parameters. The accuracy for each of the binary-encoded parameter values as parts of the candidate solution is determined by the number of bits given by the user. The accuracy of each parameter reflects also its impact with respect to the search domain containing the optimal solutions. Candidate solutions in the form binary-encoded of tool path chromosomes need to be mapped to their corresponding phenotypes in order to be evaluated by

CAM environment and further computer their results with regard to optimization criteria. To handle the number of candidate solutions; their accuracy via the number of bits for each tool path parameter and their locations in chromosomes' sequences a well-structured procedure using arrays is required. Equation 12 illustrates the array used for representing the initial population of candidate solutions C_{Pop}^{init}. In Equation 12, each of the five tool path parameters $Tlp\,\mathrm{Pr}\,m$ takes a number of bits $N_b^{Tlp\,\mathrm{Pr}\,m}{}_{i,j}$, for its accuracy in the search domain referring to the i_{th} tool path of the j_{th} population. The array to which the numbers of bits $N_b^{Tlp\,\mathrm{Pr}\,m}{}_{i,j}$ are assigned for each of tool path parameters is given in Equation 13. Finally the overall length $Lgth_i$ of each tool path chromosome in the population of solutions as well as its upper and lower levels in terms of the applicable range is assigned to another array given in Equation 14.

$$C_{Pop}^{init}=\begin{bmatrix}\{Tlp\,\mathrm{Pr}\,m_{1,1}\}_{N_b^1} & \{Tlp\,\mathrm{Pr}\,m_{1,2}\}_{N_b^2} & \{Tlp\,\mathrm{Pr}\,m_{1,3}\}_{N_b^3} & \{Tlp\,\mathrm{Pr}\,m_{1,4}\}_{N_b^4} & \{Tlp\,\mathrm{Pr}\,m_{1,5}\}_{N_b^5}\\ ..... & ..... & ..... & ..... & .....\\ \{Tlp\,\mathrm{Pr}\,m_{n,1}\}_{N_b^1} & \{Tlp\,\mathrm{Pr}\,m_{n,2}\}_{N_b^2} & \{Tlp\,\mathrm{Pr}\,m_{n,3}\}_{N_b^3} & \{Tlp\,\mathrm{Pr}\,m_{n,4}\}_{N_b^4} & \{Tlp\,\mathrm{Pr}\,m_{n,5}\}_{N_b^5}\end{bmatrix} \tag{12}$$

$$N_b^{Tlp\,\mathrm{Pr}\,m_{i,j}}=\begin{bmatrix}\{N_b^1\}_{1,j} & \{N_b^2\}_{1,j} & \{N_b^3\}_{1,j} & \{N_b^4\}_{1,j} & \{N_b^5\}_{1,j}\\ ... & ... & ... & ... & ...\\ ... & ... & ... & ... & ...\\ ... & ... & ... & ... & ...\\ \{N_b^1\}_{5,j} & \{N_b^2\}_{5,j} & \{N_b^3\}_{5,j} & \{N_b^4\}_{5,j} & \{N_b^5\}_{5,j}\end{bmatrix} \tag{13}$$

$$C_{Pop}^{init}=\begin{bmatrix}\{Lgth\}_i & u_i & l_i\\ ... & ... & ...\\ \{Lgth_n\} & u_i & l_i\end{bmatrix} \tag{14}$$

Mapping of binary-encoded tool path chromosomes to corresponding phenotypes (real parameter values) is achieved using a suitable programming function enabling the conversion of binary values to decimal ones with respect to the predetermined accuracy and the levels of applicable range. Equation 15 shows the expression applied to achieve mapping with $Tlp\,\mathrm{Pr}\,m_i$ to represent a tool path parameter; $Lgth_i$ the total length of i_{th} tool path and u_i, l the upper and lower levels respectively that define also the applicable range for the $Tlp\,\mathrm{Pr}\,m_i$ parameter; $D_{Tlp\,\mathrm{Pr}\,m_i}=[u_i, l_i]$. $BinStr$ converts directly binary-encoded numbers to decimal ones.

$$TlpPrm_i = l_i + fnc(BinStr)\times\frac{u_i - l_i}{2^{Lgth_i}-1} \tag{15}$$

Tool path chromosomes as the candidate solutions are evaluated with reference to the number of objective functions illustrating the problem. According to the nature of the optimization problem (maximization or minimization) objective values ought to be properly ranked to distinguish quality. Real-world results are quite sensitive even to small changes of tool path parameter values thus small differences among objective values should be profound enough to judge solution quality. Dealing with unnoticed differences among small objective values can lead an algorithm to select candidates randomly rather than heuristically jeopardizing thus the pure heuristic multi-objective optimization procedure of intelligent algorithms. To ensure proper selection of fitted individuals an exponential expression was therefore employed to make such small magnitudes prominent enough to distinguish them and further continue with selection. The single-point crossover has been adopted to create new generations of candidates for evaluation. The expression is given in Equation 16 with $FitSum$ to represent the sum of ranked values for candidates and $ObjVal_i$ the objective value obtained by i_{th} individual in a given population.

$$Fitted_i = FitSum\times\left[e^{\left(-ObjVal_i^2\right)}\right] \tag{16}$$

The philosophy of a virus-evolutionary genetic algorithm is entirely different when compared to other variants of intelligent algorithms which they adhere to the principles of swarm intelligence or general evolution of individuals. According to the virus theory of evolution –which is other than the popular Darwin's theory – viruses in nature can either take genetic material (DNA) from individuals to use it for their own benefit (modify their own DNA) or infect other individuals by reverse-transcribing their DNA to individuals' genome. Based on this important biological concept, viruses can serve both as "preservers" and "transmitters" of local information in an evolutionary algorithm.

In a virus-evolutionary genetic algorithm two populations; that of candidate solutions and that of viruses, co-evolve to produce and maintain efficient schemata. Crossover and mutation are responsible to generate new solutions (offspring) and maintain diversity, yet; they cannot handle schemata directly. Referring to a schema, a binary-encoded pattern is formulated to increase efficiency of the solution. Increasing a schema means an increase of local information in a given population, however; owing to proportional selection both efficient and inefficient schemata will be increased letting this way less advantageous solutions to be also promoted. On the contrary viral intelligence undertakes the creation of local information via the straightforward handling of schemata by creating virus individuals as substrings of the strings of the individuals comprising the main population. Initial viruses are created after evaluating the fitness of all candidates of the main population, as a fraction of the latter. Unlike the conventional virus-evolutionary genetic algorithm presented by Kubota (1996) that generates the viruses by randomly selecting individuals from the main population, the one proposed in this paper selects some elite individuals and some others randomly. The virus-evolutionary genetic algorithm proposed utilizes several functions so as to deliver the required results. These functions include also components that resemble the original ones presented by Kubota (1996) and new ones to further extend the algorithm's potentials.

Viral intelligence involves two operations; transduction and reverse transcription. The former operation is responsible to generate viruses as parts (substrings) of selected individuals' chromosomes whereas the latter undertakes the replacement of parts of individuals' chromosomes with those of generated viruses. In other words viruses "infect" selected individuals by subtracting parts of individuals' chromosomes and pasting their own part in that location. The initial population of tool path chromosomes C_{Pop}^{init} is randomly generated and then transduction is applied to both elite and other, randomly chosen individuals to generate the initial virus population V_{Pop}^{init}. A virus created by transducing a substring from the i_{th} chromosome of the j_{th} population is designated as Vrs_{ij} and the length of substrings corresponding to viruses' chromosomes is denoted as $VrsLgth_i$. Location $i=1$ is the starting point from which $VrsLgth_i$ is to be determined whilst Location $i_{\max}$ is to be the end point. These two locations are randomly determined and are constrained to the original host's chromosome length $Lgth_i$. While the length of individuals of the main population $Lgth_i$ is constant the length $VrsLgth_i$ of virus individuals extends up to a predetermined limit as the evolution process continues. Viruses attack to infect individuals, via reverse transcription operator for overwriting a string of a virus Vrs_{ij} to a part of an individual's string Idv_j.

Evaluation of viruses is conducted using their fitness scores $FitVrs_{i,j}$ (as it occurs also to the main population of solutions) reflecting their infection capability. Fitness is computed after the infection of Idv_j by Vrs_{ij} as Equation 17 indicates:

$$FitVrs_{i,j} = FitInfIdv_j - FitIdv_j \quad (17)$$

The result of Equaiton 17 shows the difference between the two fitness values of individual Idv_j before and after infection by Vrs_{ij}. Vrs_{ij} might have the chance to infect more than one individual -let S be the sum of successfully infected individuals- thus $FitVrs_{i,j}$ exhibits the improvement of fitness values of all infected individuals and is as Equation 18 determines:

$$FitVrs_i = \sum_{j \in S} FitVrs_{i,j} \quad (18)$$

The advantageous infection of a virus Vrs_{ij} is measured using the $InfForce_{i,g}$ indicator where i is the index of the virus Vrs_{ij} and g the current generation of individuals that applies its infection. $InfForce_{i,g}$ is dependent on the result of $FitVrs_i$ and is compared to the one attained by the virus Vrs_{ij} in a previous generation. If its value is lower than the one attained in the previous generation ($InfForce_{i,g-1}$) then transduction is applied to produce a new virus. If the value of $InfForce_{i,g}$ is greater than $InfForce_{i,g-1}$ then the virus Vrs_{ij} increases its scheme by partially transducing a new substring from the infected individual.

In conventional virus-evolutionary genetic algorithm the infection rate of viruses is controlled with regard to their fitness score $FitVrs_i$ and the infection rate of viruses $InfRateVrs_{ij}$ where $0 \le InfRateVrs_i \le 1$ for self-adaptively adjusting the search between exploitation and exploration. In the algorithm proposed in this work $InfRateVrs_{ij}$ may

be restricted to new intervals if the algorithm fails to increase effective schemata. Thus, $InfRateVrs_{i\,j}$ may be constrained to a minimum value such that $0 \le MinInfRateVrs_i \le 0.5$ and a maximum value such that $0.5 \le MaxInfRateVrs_i \le 1$. By introducing a two-fold infection rate, self-adaptation in terms of exploitation and exploration is controlled according to the engineering problem's nature using discrete operational intervals. The main population of candidate solutions and the secondary population of viruses are simultaneously evolved to create robust and qualitative solutions for the optimization problem at hand. The combination of individuals and viruses enables the algorithm to create new solutions as a "horizontal propagation" which is beneficial for passing local information to new solutions from previous ones. In addition, viruses may vertically transmit their information to the strings of individuals, thus; maintaining local information from generation to generation as a "vertical inheritance". As a result fast global search is accompanied to local information as well to satisfy both exploration and exploitation. Figure 3 illustrates the workflow of the proposed virus-evolutionary genetic algorithm of the optimization methodology presented in the paper.

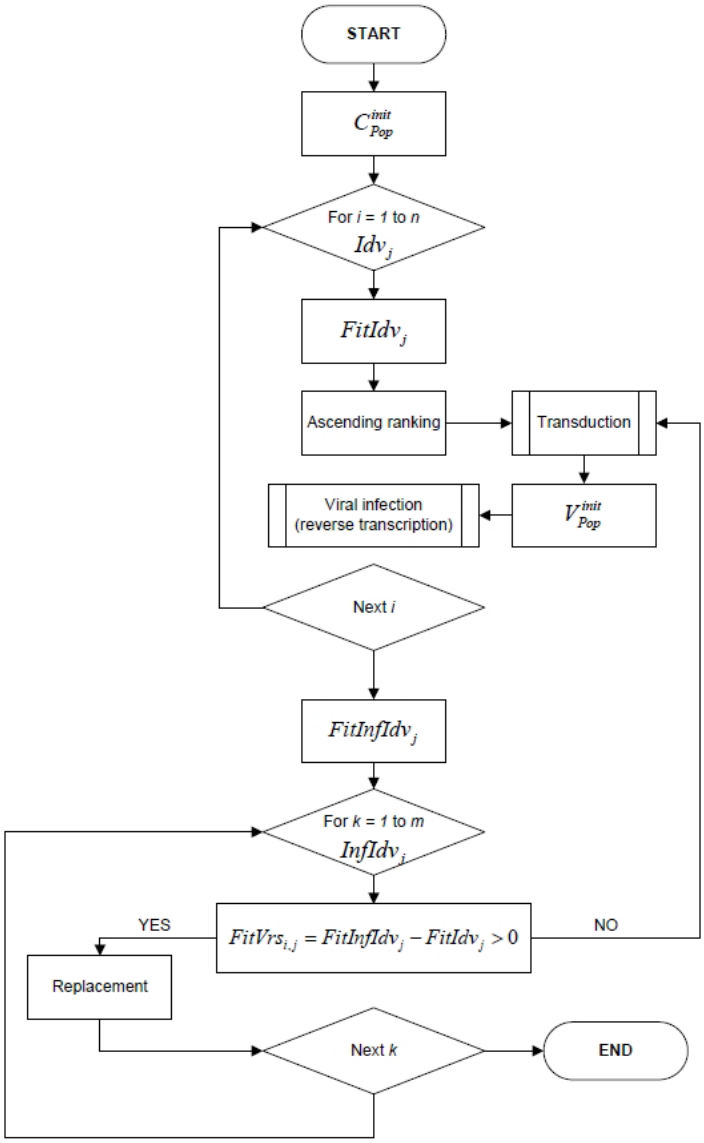

Figure 3. Workflow of the proposed virus-evolutionary genetic algorithm.

4.2 Steps for achieving optimal tool path generation for sculptured surface machining

Step 1: Inputs of values for tool path parameters according to prescribed minimum-maximum intervals and number of accuracy digits for binary representation. Tool path individuals are initialized according to the predefined number of candidate solutions for evaluation.
Step 2: Automated evaluation of candidate tool paths using their real value representation after binary encoding via the aforementioned interaction programming module. Real values from binary representation are loaded to CAM system's

machining modeling interface updating thus parameters of the cutting strategy. Tool path computation is automatically conducted to extract CL data whose coordinates are imported to CAD interface containing the target sculptured surface. A grid of CL points in u and v parametric directions is then formulated to represent the tool path (Figure 4a). With reference to CL data, projections normal to part's curvature are sequentially performed to enable vector algebra computation in terms of the magnitudes of point-to-point 3D lengths, local curvatures and finally local chordal deviations. In the methodology, gouge detection (Xu et al. 2002) is achieved by enabling the corresponding function for restricting accessibility of a tool should its configuration does not allow fitting its inclined posture to part's curvature. In the case of gouging, local surfacic regions are left without any CL points for the tool to interpolate and the corresponding tool path is penalized by assigning a large value for its fitness loosing this way its potentials to be chosen as candidate solution in next genes (Figure 4b).

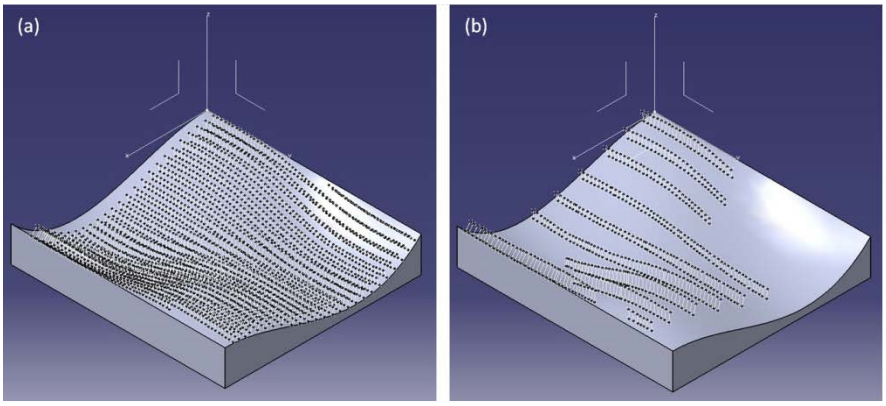

Figure 4. Grids of CL points on a given sculptured surface: (a) feasible tool path; (b) penalized tool path owing to gouging.

The procedure of automatically handling CAM system's utilities in the case of sculptured surface CNC machining optimization is given in Figure 5.

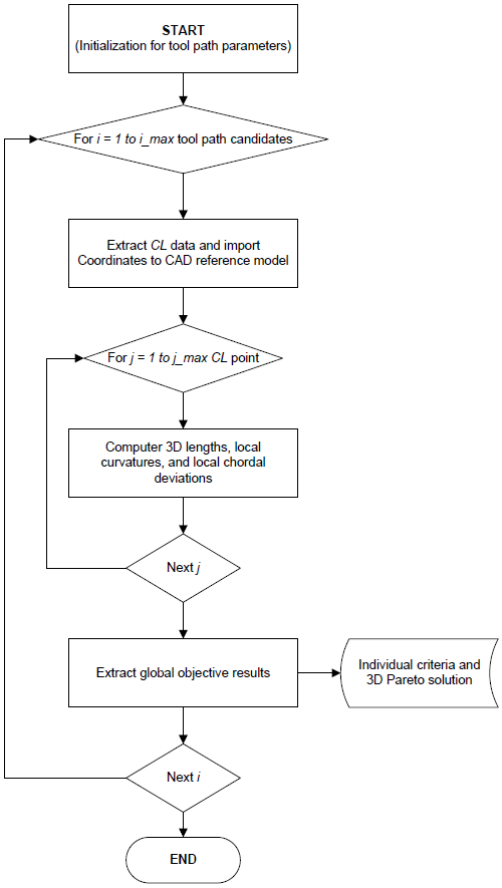

Figure 5. Workflow of the interaction programming module handling CAM system's properties.

Step 3: Each tool path candidate is evaluated and then ranked in ascending order according to its fitness score. Selection and crossover are then performed to choose elite tool paths for constituting the next generation of candidates. One-point crossover is selected for the reason that viral operators applied later change schemes to a large extend and good solution damage may occur. At this point a second population of virus individuals is created as a fraction of the number of the main tool path population. Viruses are created as substrings by stings of the hosts (candidate tool paths of the main population) whereas they are prompted to come from both the elite and randomly selected individuals. Whilst the string length of candidate tool paths is constrained to a fixed value, the length of viruses may vary as the evolution continues. Thus, a significant advantage is obtained dealing with the increase of effective schemata towards the ultimate goal of finding the best tool path since viruses are technically the carriers of local information preventing the algorithm from being trapped. In other words viruses tend to increase schemata in the main population of tool paths directly via viral infection. Viral infection operation follows the procedure described in sub-section 4.1.

Step 4: Next generation involves tool path candidates as well-fitted offspring and successfully infected individuals. These individuals are transformed to their real value representation for further processing in CAM software. The system produces the CL data for the new tool path and the procedure is repeated from step 2. The proposed methodology terminates the optimization process after all evaluations as per the number of individuals and generations whereas optimal tool path parameters are further utilized to extract the CL file for post-processing and its final execution in the CNC machine tool in the form of a standard ISO code.

4.3 Comparison using intelligent heuristics

A number of state-of-the art multi-objective evolutionary algorithms (MOEAs) have been selected to compare and validate the performance of the proposed virus-evolutionary GA integrating the proposed methodology. These MOEAs are multi-objective multi-verse optimizer (MOMVO); multi-objective ant lion optimizer (MOALO); multi-objective grey wolf optimizer (MOGWO) and multi-objective dragonfly algorithm (MODA), (Mirjalili et al., 2016a; 2016b; 2017a; 2017b) as well as evolutionary multi-objective optimization algorithm (evMOGA) developed by Martinez et al., 2009.

All MOEAs have been developed in MATLAB® and their applications may be found in the literature presented above. For the sake of rigorous comparisons among different versions of multi-objective evolutionary algorithms (MOEAs) regression equations were derived with respect to the full factorial experiments and ANOVA analysis conducted for the benchmark sculptured surfaces presented in the paper. Algorithm-specific operators were kept as per their inventors' recommendations for best performance whereas 10 individuals were determined to be evolved for 50 generations.

The regression models per benchmark surface formulated a three-objective function. Thereby, for each MOEA and benchmark surface, 10 runs were conducted to test best result; average of solutions and standard deviation. The study considers the time-consuming effort and computational burden of the approach when operating using CAM software and this justifies the aforementioned settings. During the tests all MOEAs were operated according to the last best population to investigate to what extend the proposed optimal solution could be improved. The following tables (Tables 2, 3, 4 and 5) summarize the results from the mean values of best; average and standard deviation for all MOEAs and test surfaces. It is clear that, in all cases the proposed virus-evolutionary GA (MOVEGA) is superior to its rest competitors.

Table 2. Optimization results for MOEAs with regard to benchmark sculptured surface 1 (SS-1).

Algorithm/Performance metric	MOVEGA	MOGA	MOMVO	MOALO	MOGWO	MODA	evMOGA
$\overline{\min_{10} ffp}$	0.513262	0.520201	0.546173	0.558030	0.546939	0.545884	0.630427
$\overline{\max_{10} ffp}$	1.470172	1.342820	0.853937	0.998737	1.002916	0.929008	0.874105
$\overline{avg_{10} ffp}$	0.624935	0.609852	0.637445	0.688532	0.657111	0.631945	0.697858
$\overline{stdev_{10} ffp}$	0.069913	0.088636	0.068371	0.097722	0.102120	0.078314	0.059436

Table 3. Optimization results for MOEAs with regard to benchmark sculptured surface 2 (SS-2).

Algorithm/Performance metric	MOVEGA	MOGA	MOMVO	MOALO	MOGWO	MODA	evMOGA
$\overline{\min_{10} ffp}$	1.085090	1.092930	1.193373	1.209252	1.242398	1.272818	1.390233
$\overline{\max_{10} ffp}$	2.052383	2.383725	2.363889	2.460966	2.558104	2.326633	2.217181
$\overline{avg_{10} ffp}$	1.154107	1.232038	1.611356	1.667946	1.784325	1.696424	1.739283
$\overline{stdev_{10} ffp}$	0.083831	0.167760	0.275046	0.249926	0.299667	0.232281	0.210267

Table 4. Optimization results for MOEAs with regard to benchmark sculptured surface 3 (SS-3).

Algorithm/Performance metric	MOVEGA	MOGA	MOMVO	MOALO	MOGWO	MODA	evMOGA
$\overline{\min_{10} ffp}$	0.410796	0.417924	0.466598	0.454044	0.461560	0.457721	0.620104
$\overline{\max_{10} ffp}$	1.308863	1.303210	1.076429	1.295356	1.266048	1.256374	1.174027
$\overline{avg_{10} ffp}$	0.426087	0.498082	0.739844	0.847859	0.812907	0.790610	0.789919
$\overline{stdev_{10} ffp}$	0.080034	0.142008	0.172423	0.212407	0.217128	0.243510	0.131833

Table 5. Optimization results for MOEAs with regard to benchmark sculptured surface 4 (SS-4).

Algorithm/Performance metric	MOVEGA	MOGA	MOMVO	MOALO	MOGWO	MODA	evMOGA
$\overline{\min_{10} ffp}$	0.848587	0.879023	0.876424	0.916828	0.856792	0.907482	1.084765
$\overline{\max_{10} ffp}$	1.599503	1.757536	1.406039	2.080599	1.896094	1.789422	1.594121
$\overline{avg_{10} ffp}$	0.861147	1.078813	1.064821	1.571718	1.199209	1.173132	1.267003
$\overline{stdev_{10} ffp}$	0.060315	0.123829	0.166284	0.314386	0.243378	0.231146	0.143471

Note that the same algorithm was operated without deploying its virus operators (reverse transcription and transduction) to observe their contribution to the proposed heuristic when employing them. Under this perspective the proposed algorithm is named as MOGA. Figure 6 illustrates the comparisons made among the MOEAs in terms of their number of executions (runs) per each benchmark surface in terms of the minimum (best) result obtained. It can be seen that the proposed algorithm not only contributes to the optimization process by lowering the minimum result but maintains repeatability in reaching it when multiple trials are performed.

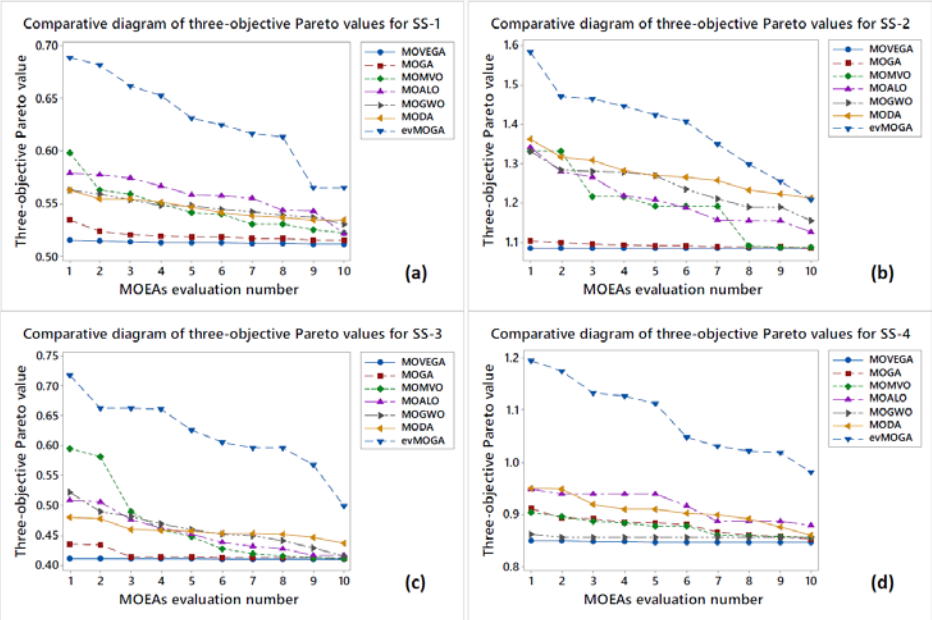

Figure 6. Comparative diagrams to examine the overall performance of the proposed algorithm on the optimization process with regard to the test surfaces: (a) SS-1; (b) SS-2; (c) SS-3; (SS-4).

5. Methodology validation

To validate the proposed methodology a benchmark sculptured surface was selected for actual 5-axis CNC machining with the goal of rigorously comparing the results to those already available in the literature, for exactly the same problem. To provide a link between our research and actual industrial manufacturing systems a post-processing engine was developed. The post-processing engine takes into account the technical specifications of the 5-axis machine tool finally used as well as the properties of the CNC unit such as the CL data sampling time. It also constitutes a part of the interaction programming module with the difference that it is applied only in the end, for translating CL file commands to ISO code. It is capable of achieving proper feed rate adaptation with respect to the local curvatures and resultant chordal deviations (Lu, Ding and Zhu 2016; Moodleah, Bohez and Machanov 2016). Its accuracy and reliability was

verified using *CG Tech® Vericut® 7.1* NC verification software. Results were compared to those obtained by employing a commercially available Post-processing engine embedded to CAM system for the same part.

The benchmark sculptured surface selected was a second-order; open-form parametric surface extensively tested by several researchers (Lu, Ding and Zhu 2017; Fountas et al. 2017; Gan et al. 2016; Xu et al. 2010; Warkentin, Ismail and Bedi 2000b; Rao, Ismail and Bedi 1997). The following equation was adopted to construct the surface whilst its result is depicted in Figure 7a. The tool path applied is depicted in Figure 7b.

$$S(u,v)=\begin{bmatrix} -94.4+88.9v+5.6v^2 \\ -131.3u+28.1u^2 \\ a_1+a_2 \end{bmatrix}, \begin{Bmatrix} a_1=5.9(u^2v^2+u^2v)-3.9v^2u+76.2u^2 \\ a_2=6.7v^2-27.3uv-50.8u+25v+12.1 \end{Bmatrix} \quad (19)$$

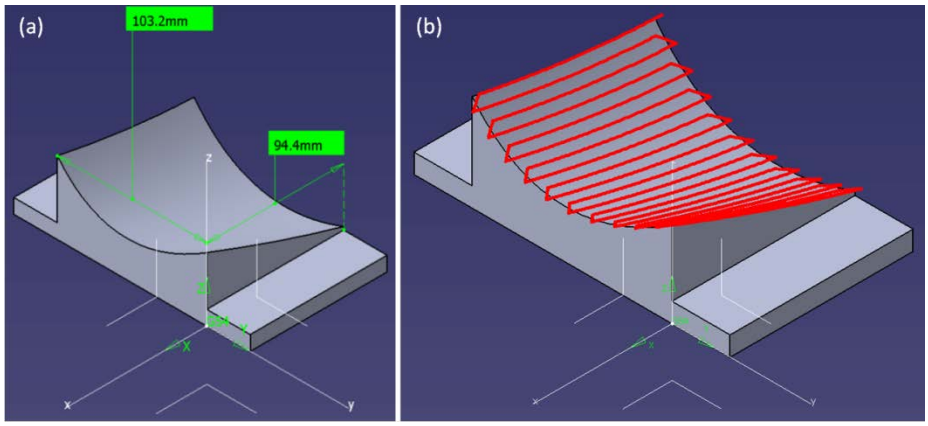

Figure 7. Benchmark surface for actual cutting experiments: (a) Benchmark sculptured surface; (b) multi-axis swept cut tool path.

The optimal recommended values for tool path parameters were 6.68 mm for step over; 3.379 degrees for lead angle; 0.027 degrees for tilt angle and 6.338×10^{-3} mm for maximum discretization step. Cut tolerance was set equal to 0.01mm as proposed for finishing molds and dies (Segonds et al. 2017). Machining time was approximately 1min, 24sec. Early inspections shown that a remarkable smoothness was obtained in both directions (X and Y axes).

A two-fold inspection was conducted to the machined part. The former inspection refers to the examination of the machining error owing to scallop height and conducted to the resultant machining strips perpendicular to X-axis. The latter inspection refers to the examination of the machining error owing to chord error and conducted to the resultant machining strips parallel to X-axis. For the first inspection type, four surface profile sections were evaluated perpendicular to feed direction (X-axis) as per the proposals of Fountas et al. 2017; Gan et al. 2016; Xu et al. 2010; Warkentin, Ismail and Bedi 2000b; Rao, Ismail and Bedi 1997. The profile sections were produced by moving Z-Y plane towards positive values referring to X-axis, with reference to the machining axis system (G54). These section cuts were done at X= -5mm; X= -30mm; X= -60mm and X= -90mm and measured by a CMM (Figure 8a and 8b). For the second inspection type, a *Taylor-Hobson® Surtronic 3+* roughness tester was used for examining the continuity among sequentially connected postures of CL data referring to X-axis feed-forward direction. Except from the convenient side-effect of observing physical quality, the roughness tester was used mainly under the assumption that, with a continuous travelling step by the instrument's stylus, the "roughness" diagram would give a good depiction for commenting on the uniformity of machining error towards feed direction (and consecutively the local fluctuations of connected tool path postures producing that error). However high accuracy in terms of the stylus's travelling is impossible to be achieved owing to the part's curvature. Figure 8c shows the process of testing three of the machining strips as representative to the machining error owing tool interpolation. Two machining strips selected close to the part's curved edges referring to Y direction and a third one was selected in the middle. Proper positioning was ensured to reduce the process-related errors to the best possible extend.

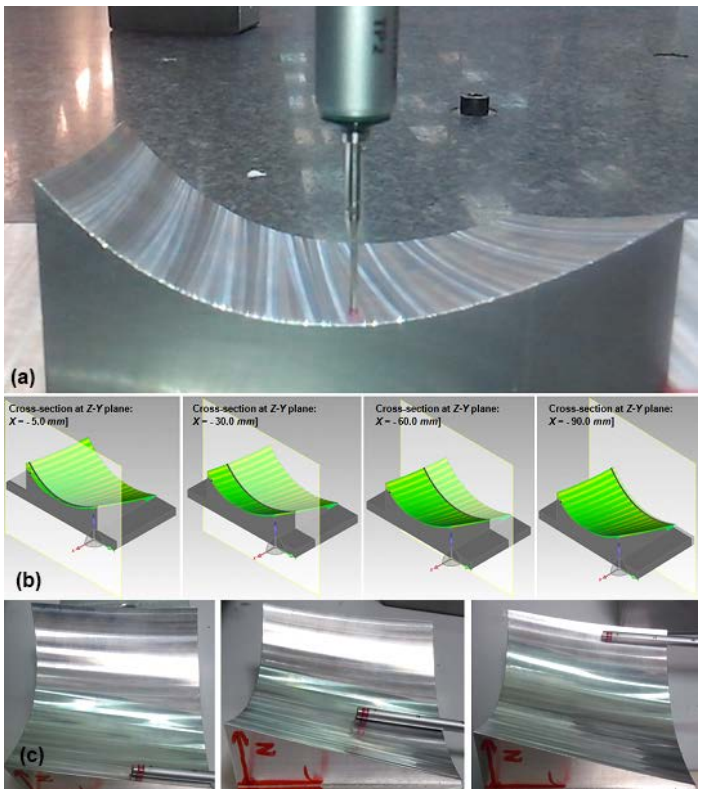

Figure 8. Two-fold inspection process for the machined surface: (a) CMM inspection equipment; (b) cross-sections for CMM inspection, X=-5mm; X=-30mm; X=-60mm and X=-90mm; (c) Form error testing approach using a roughness tester travelled on three machining strips.

Figure 9a and Figure 9b give the simulated and the experimental measurements for the aforementioned cross-section X= -5mm; Figure 9c and Figure 9d give the simulated and the experimental measurements for cross-section X= -30mm; Figure 9e and Figure 9f give the simulated and the experimental measurements for cross-section X= -60mm and Figure 9g and Figure 9h give the simulated and the experimental measurements for cross-section X= -90mm. It can be seen that experimental CMM measurements are in agreement with their corresponding simulated ones and scallop height is between the tolerance zone of ±0.01mm as suggested. Noticeable error is only observed in the two guide curves close to X= -5mm and X= -90mm owing to cutting tool's vibrations in its approach (X= -5mm) and departure (X= -90). In general if process-related errors (tool deflection, stability, etc) and CMM positioning errors are neglected, surface deviation still complies with the preset tolerance. By considering the general trend of both simulated and experimental measurements it can be supported that the overall machining error is uniformly distributed at least referring to Y-direction perpendicular to feed. Machining strips were the largest possible given the cutting tool employed (Warkentin, Ismail and Bedi 2000b).

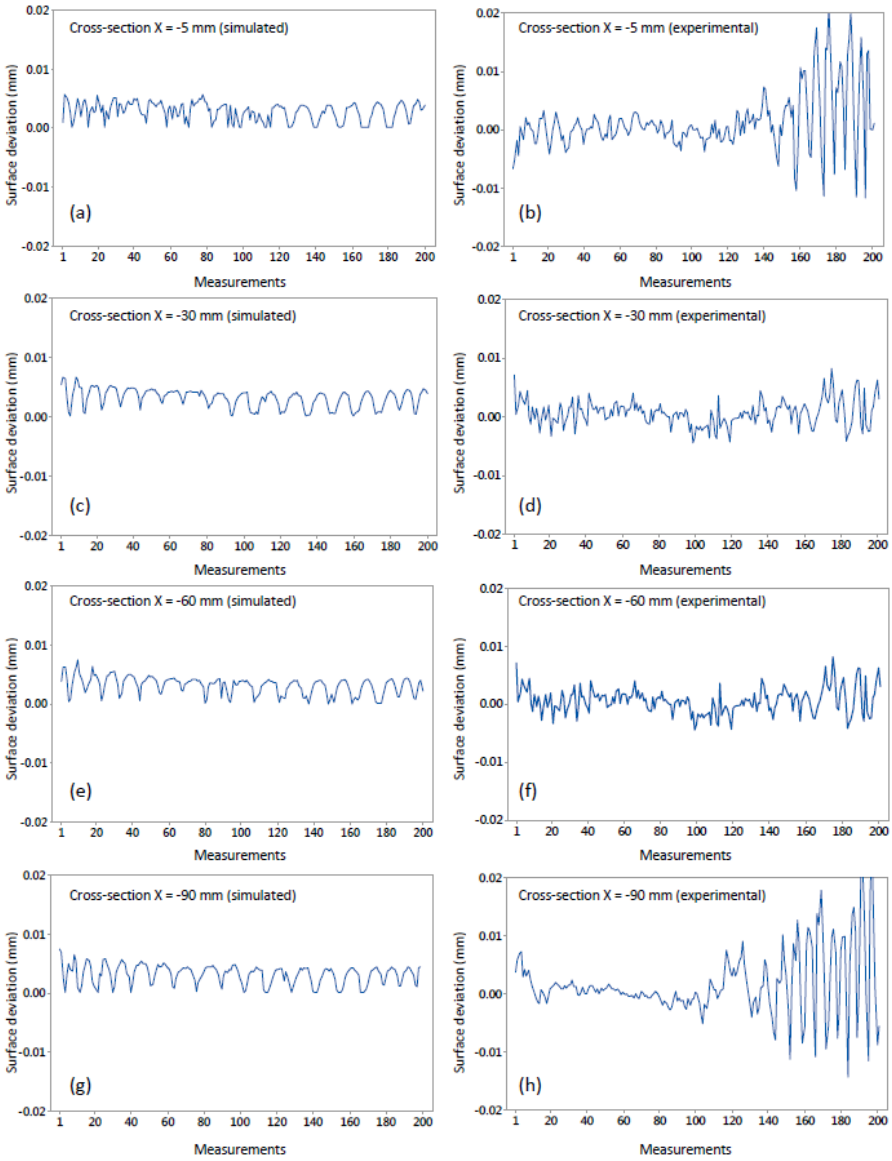

Figure 9. Comparison of results among simulated and CMM-inspected cross-sections: (a) X=-5mm simulated; (b) X=-5mm experimental; (c) X=-30mm simulated; (d) X=-30mm experimental; (e) X=-60mm simulated; (f) X=-60mm experimental; (g) X=-90mm simulated; (f) X=-90mm experimental.

"Roughness" plots presented remarkably uniform profiles of inclined toroidal connected postures. This is observed by the characteristical "error" lying underneath a toroidal tool with the form of 'w' shaped valleys (Warkentin, Ismail and Bedi 2000b; Fan et al. 2013). In the plots, most of the 'w'shaped errors have quite the same figure in the measuring length of 0.8mm whereas this result can be generalized also to the rest of the surface regions revealing insignificant variation towards the connected tool path postures. Figures 10a, 10b and 10c illustrate this result for three selected machining strips.

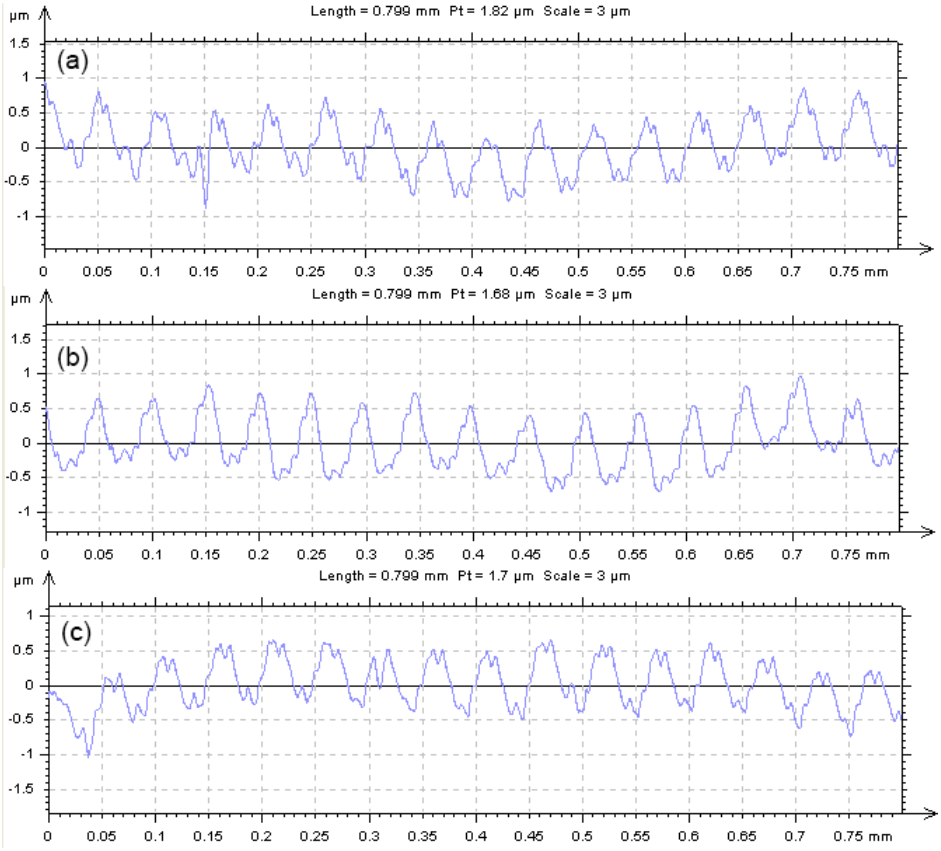

Figure 10. Representative machining error profiles corresponding to Figure 8c: (a) profile obtained from the left machining strip; (b) profile obtained from the central machining strip; (c) profile obtained from the right machining strip.

From the consistency of simulated and inspected results referring to the machining error and tool path postures it can be supported that the proposed optimization methodology can provide promising outputs for accurate and productive tool paths. By examining the aforementioned results referring to the machining error and tool path time obtained by the implementation of the proposed methodology, it can be stated that sculptured surface tool path parameters may be stochastically optimized to generate as much cutting tool points as needed to satisfy the requirement of tool path smoothness; low machining error and productivity.

7. Conclusions and future perspectives

Successful optimization for sculptured surface CNC machining tool paths does not depend only to novel intelligent algorithms' applications but also to the proper problem formulation reflected by the design of optimization criteria and their expression; either individually assessing productivity, or surface quality, or both as a trade-off problem. To solidify this important concept and to further contribute to the already well-established research field of optimized sculptured surface tool path planning, the current work presented a methodology for optimizing sculptured surface CNC tool paths using an intelligent algorithm and a CAM system. The problem suggests the averages of machining error and standard deviation as trustworthy representations for globally optimizing the problem with regard to tool path smoothness, whilst local variations are also considered. The problem is handled through an automated fashion and with the application of a virus-evolutionary genetic algorithm for avoiding local trapping towards its convergence. A major limitation of the proposed work is the computational time needed to handle manufacturing software entities, (i.e. simulation tools). However owing to the progress on new hardware and software for computerized systems aim to support production, this shortcoming may be reduced to a considerable fraction. It should be mentioned that the work presented does not include the mechanics of processes. Even though this is not within the primarily objectives of the current research it should be taken into account to deliver even more reliable results for solving the generalized sculptured surface machining optimization problem. As a major future perspective the authors are looking forward to conduct research concerning other intelligent machining essentials involving machining setup planning and minimization of vibrations during cutting. The authors are to propose functions for characterizing setup generation, operation sequence and setup sequence to be handled by, either the same heuristic presented in this paper, or an enhanced version of it. Intelligent setups will be assessed with regard to constraints such as fixtures and jigs, precedence

constraints in machining features as well as tolerance relations. The objective function will probably follow a “minimum spanning tree” or a “travelling salesman” mapping for sequential evaluations until a stopping criterion is met. In addition, actual experiments are to be conducted to collect data for capturing the dynamic process behavior of sculptured surface CNC machining and try to solve a multi-objective optimization problem for compensating errors, process stability, machining performance and other important process-related errors. Step-NC functionality is also considered to constitute a research objective so as to try “on-line” optimization efforts.

Disclosure statement

No potential conflict of interest was reported by the authors.

References

Agrawal, R.K., D.K. Pratihar, and R. Choudhury. 2006. “Optimization of CNC isoscallop free form surface machining using a genetic algorithm.” *International Journal of Machine Tools and Manufacture* 46(7):811-819.

Amaral A.R.S. 2018. “A mixed-integer programming formulation for the double row layout of machines in manufacturing systems”. International Journal of Production Research, DOI: 10.1080/00207543.2018.1457811.

Chansombat, S., P. Musikapun, P. Pongcharoen, and C. Hicks. 2018. “A Hybrid Discrete Bat Algorithm with Krill Herd-based advanced planning and scheduling tool for the capital goods industry.” International Journal of Production Research, DOI: 10.1080/00207543.2018.1471240.

Djebali, S., S. Segonds, J-M. Redonnet, and W. Rubio. 2015. “Using the Global Optimization Methods to Minimise the Machining Path Length of the Free-form Surfaces in Three-axis Milling.” *International Journal of Production Research* 53(17):5296-5309.

Fan, W., P. Ye, H., Zhang, C. Fang, and R. Wang. 2013. “Using rotary contact method for 5-axis convex sculptured surfaces machining.” *International Journal of Advanced Manufacturing Technology* 67:2875-2884.

Fard, M. J. B., and H. Y. Feng. 2011. “New Criteria for Tool Orientation Determination in Five-axis Sculptured Surface Machining.” *International Journal of Production Research* 49(20):5999-6015.

Fountas, N.A., R. Benhadj-Djilali, C.I. Stergiou, and N.M. Vaxevanidis. 2017. “An integrated framework for optimizing sculptured surface CNC tool paths based on direct software object evaluation and viral intelligence.” *Journal of Intelligent Manufacturing,* DOI: 10.1007/s10845-017-1338-y.

Gan, Z., Z. Chen, M. Zhou, J. Yang, and S. Li. 2016. “Optimal cutter orientation for five-axis machining based on mechanical equilibrium theory.” *International Journal of Advanced Manufacturing Technology* 84(5-8):989-999.

Gray P.J., S. Bedi, and F. Ismail. 2005. “Arc-intersect method for 5-axis tool positioning.” *Computer-Aided Design* 37(7):663-674.

Gray, P., S. Bedi, and F. Ismail. 2003. “Rolling ball method for 5-axis surface machining.” Computer-Aided Design 35: 347-357.

Gray, P.J., F. Ismail, and S. Bedi. 2004. “Graphics-assisted Rolling Ball Method for 5-axis surface machining.” *Computer Aided Design* 36(7):653-663.

Jensen, C.G., and D.C. Anderson. 1993. “Accurate tool placement and orientation for finish surface machining.”*Journal of Design and Manufacturing* **3**(4):251-261.

Kubota, N., T. Fukuda, and K. Shimojima. 1996. “Virus-evolutionary algorithm for a self-organizing manufacturing system.” *Computers and Industrial Engineering* 30(4):1015-1026.

Lamikiz, A., L.N., López de Lacalle, J.A. Sanchez, and M.A. Salgado. 2005. “Cutting force integration at the CAM stage in the high speed milling of complex surfaces.” *International Journal of Computer Integrated Manufacturing* 18(7):586-600.

Li, Y., C.-H., Lee, and J. Gao. 2015. “From Computer-Aided to Intelligent Machining: Recent Advances in CNC Machining Research.” *Proceedings of the Institution of Mechanical Engineers, Part B: Journal of Engineering Manufacture* 229(7):1087-1103.

Liang, Y-C., and J. R.C. Juarez. 2016 “A novel metaheuristic for continuous optimization problems: Virus optimization algorithm.” *Engineering Optimization* 48(1): 73-93.

López de Lacalle, L.N. , A. Lamikiz, J. Muñoa and J.A. Sánchez. 2005. “The CAM as the centre of gravity of the five-axis high speed milling of complex parts.” *International Journal of Production Research* 43(10):1983-1999.

Lu, C., X. Li, L. Gao, W. Liao, and J. Yi. 2017. “An effective multi-objective discrete virus optimization algorithm for flexible job-shop scheduling problem with controllable processing times.” *Computers and Industrial Engineering* 104:156-174.

Lu, Y. A., Y. Ding, and L. M. Zhu. 2016. “Simultaneous Optimization of the Feed Direction and Tool Orientation in Five-axis Flat-end Milling.” *International Journal of Production Research* 54(15):4537-4546.
Lu, Y., Y. Ding, and L. Zhu. 2017. “Tool path generation via the multi-criteria optimization for flat-end milling of sculptured surfaces.” *International Journal of Production Research* 55(15):4261-4282, DOI: 10.1080/00207543.2016.1232496.
Manav, C., H. S. Bank, and I. Lazoglu. 2013. “Intelligent Toolpath Selection via Multi-criteria Optimization in Complex Sculptured Surface Milling.” *Journal of Intelligent Manufacturing* 24(2):349-355.
Martínez, M., J.M. Herrero, J. Sanchis, X. Blasco, and S. García-Nieto. 2009. “Applied Pareto multi-objective optimization by stochastic solvers.” *Engineering Applications of Artificial Intelligence* 22:455-465.
Mirjalili, S. 2016b. “Dragonfly algorithm: a new meta-heuristic optimization technique for solving single-objective, discrete, and multi-objective problems.” *Neural Computing and Applications* 27(4):1053-1073.
Mirjalili, S., P. Jangir, and S. Saremi. 2017b. “Multi-objective ant lion optimizer: a multi-objective optimization algorithm for solving engineering problems.” *Applied Intelligence* 46(1):79-95.
Mirjalili, S., P. Jangir, S.Z. Mirjalili, S. Saremi, and I.N. Trivedi. 2017a. “Optimization of problems with multiple objectives using the multi-verse optimization algorithm.” *Knowledge-Based Systems* 134:50-71.
Mirjalili, S., S. Saremi, S.M. Mirjalili, and L.S. Coelho. 2016a. “Multi-Objective grey wolf optimizer: A novel algorithm for multi-criterion optimization.” *Expert Systems with Applications* 47(1):106-119.
Mohammad, R-M, M. Mohammadi, J-Y. Dantan, A. Siadat, and R. Tavakkoli-Moghaddam. 2018. “A review on optimisation of part quality inspection planning in a multi-stage manufacturing system.” *International Journal of Production Research*”, DOI: 10.1080/00207543.2018.1464231.
Moodleah, S., and S. S. Makhanov. 2015. “5-Axis Machining Using a Curvilinear Tool Path Aligned with the Direction of the Maximum Removal Rate.” *International Journal of Advanced Manufacturing Technology* 80(1): 65-90.
Moodleah, S., E. J. Bohez, and S. S. Makhanov. 2016. “Five-axis Machining of STL Surfaces by Adaptive Curvilinear Toolpaths.” *International Journal of Production Research* 54(24):1-34.
Mordkoff, Toby J. 2015 “The Assumption(s) of Normality.”
Rao, N., F. Ismail, and S. Bedi. 1997. “Tool path planning for five-axis machining using the principal axis method.” *International Journal of Machine Tools and Manufacture* 37 (7):1025-1040.
Redonnet, J. M., A. G. Vázquez, Michel, A.T., and S. Segonds. 2016. “Optimisation of free-form surface machining using parallel planes strategy and torus milling cutter.” *Proceedings of the Institution of Mechanical Engineers, Part B: Journal of Engineering Manufacture* DOI: 10.1177/0954405416640175.
Redonnet, J. M., S. Djebali, S. Segonds, J. Senatore, and W. Rubio. 2013. “Study of the effective cutter radius for end milling of freeform surfaces using a torus milling cutter.” *Computer-Aided Design* 45(6): 951-962.
Roman, A., E. Barocio, J. C. Huegel, and S. Bedi. 2015. “Rolling ball method applied to 3½-axis machining for tool orientation and positioning and path planning.” *Proceedings of the Institution of Mechanical Engineers, Part B: Journal of Engineering Manufacture* 7(12): 1-12.
Segonds, S., P. Seitier, C. Bordreuil, F. Bugarin, W. Rubio, and J-M. Redonnet. 2017. “An analytical model taking feed rate effect into consideration for scallop height calculation in milling with torus-end cutter.” *Journal of Intelligent Manufacturing*, DOI 10.1007/s10845-017-1360-0.
Ulker, E.,M.E. Turanalp, and H.S. Halkaci. 2009. “An artificial immune system approach to CNC tool path generation.” *Journal of Intelligent Manufacturing* 20:67-77.
Vickers, G.W., and K. Quan. 1989. “Ball-mills versus end-mills for curved surface machining.” *Journal of Engineering for Industry* 111(2):22-26.
Warkentin, A., F. Ismail, and S. Bedi. 2000a. “Multi-point Tool Positioning Strategy for 5-Axis Machining of Sculptured Surfaces.” Computer Aided Geometric Design 17 (1): 83-100.
Warkentin, A., F. Ismail, and S. Bedi. 2000b. Comparison between multipoint and other 5-axis tool position strategies.” *International Journal of Machine Tools and Manufacture* 40(2):185-208.
Xu, R., C. Zhitong, C.Wuyi, W. Xianzhen, and Z. Jianjun. 2010. “Dual drive curve tool path planning method for 5-axis NC machining of sculptured surfaces.” *Chinese Journal of Aeronautics* 23:486-494.
Xu, X.J., C. Bradley, Y.F. Zhang, H.T. Loh, and Y.S. Wong. 2002. “Tool-path generation for five-axis machining of free-form surfaces based on accessibility analysis.” *International Journal of Production Research* 40(14):3253-3274.
Zeroudi, N., M. Fontaine, and K. Necib. 2012. “Prediction of cutting forces in 3-axes milling of sculptured surfaces directly from CAM tool path.” *Journal of Intelligent Manufacturing* 23(5):1573-1587.